ISSN(PRINT) : 2320 -1967
ISSN(ONLINE) : 2320 -1975

GLOBAL SCIENTIFIC INC.

ChemXpress

ORIGINAL ARTICLE

CHEMXPRESS 9(2), 156-171, (2016)

Phenoxo- and azido-bridged complexes with N_2OS_2 Schiff-base ligand; synthesis, spectral investigation and bacterial activity

Talib H.Mawat, Mohamad J.Al-Jeboori*

Department of Chemistry, College of Education for Pure Science (Ibn Al-Haitham), University of Baghdad, P.O. Box 4150, Adhamiyah, Baghdad, (IRAQ)
E-mail: mohamadaljeboori@yahoo.com
Received : 29th March, 2015 ; Revised : 18th August, 2015 ; Accepted : 26th August, 2015

Abstract : A series of phenoxo- and azido-bridged complexes with potentially binucleating N_2OS_2 multidentate Schiff-base ligand (HL) are reported. The condensation reaction of 2,6-diformyl-4-methyl-phenol with 2-(4-amino-5-mercapto-4H-1,2,4-triazol-3-yl)phenol in a 1:2 mole ratio afforded the preparation of the new Schiff-base ligand 4'-(((1E,1'E)-(2-hydroxy-5-methyl-1,3-phenylene)bis(methanylylidene))bis(azanylylidene))bis(5-(2-hydroxyphenyl)-2,4-dihydro-3H-1,2,4-tr- iazole-3-thione. The reaction of the ligand with Cr(III), Mn(II), Fe(II) Co(II), Ni(II), Cu(II), Zn(II), Cd(II) and Hg(II) metal ions resulted in the formation of binucleating phenoxo-bridged complexes, of general formula $[Cr_2L(H_2O)_2Cl_4]Cl$, $[M_2L(H_2O)_4Cl_2]Cl$, $K[Cu_2L(H_2O)_2Cl_4]$, $[M'_2LCl_2]Cl(H_2O)$ and $K[Zn_2LCl_4]$ (M= Mn(II), Co(II) and Ni(II); M'= Fe(II) or Cd(II); M'= Hg(II), H_2O= 0). The reactivity studies of the phenoxo-bridged binucleating complexes toward azido moiety were also investigated, which gave tetranuclear μ-1,1-azido-bridged complexes of the general formula $[Cr_2L(N_3)_4]Cl(H_2O)_2$ and $Na[M_2L(N_3)_4](H_2O)_2$ (M= Mn(II), Fe(II), Co(II), Ni(II), Cu(II), Zn(II), Cd(II) and Hg(II). The mode of bonding and predicted geometry of complexes were determined through physico-chemical and spectroscopic methods. These analytical and physical studies for the phenoxo-bridged binucleating complexes revealed octahedral and tetrahedral geometries about (Mn(II), Co(II) and Ni(II)) and (Fe(II), Cd(II) and Hg(II)) ions, respectively. However, a five-coordinate structure is proposed for the Zn(II) complex. The formation of octahedral geometries about metal centre has been suggested for the tetranuclear azido-bridged complexes. The ligand and its metal complexes were screened against Gram negative bacterial strains *Escherichia coli (E. coli), Pseudomonas aeruginosa and Bacillus sabtuius* and Gram positive bacterial strain *Staphylococcus aureus* that revealed the metal complexes become more potentially resistive to the microbial activities as compared to the free ligand.

Keywords : Schiff-base ligand; Transition metal complexes; Reactivity reaction; Structural study; Bacterial activity.

ORIGINAL ARTICLE

INTRODUCTION

Schiff-bases are an interesting organic species that attracted organic, inorganic and bioinorganic chemists. They played a significant role in the development of chemistry, in particular coordination chemistry. Schiff-bases are excellent chelating agents that have the ability to form stable compounds, with transition and representative elements[1, 2]. They have potential applications in biomedical[3], biomimetic[4], analytical chemistry[4], coordination chemistry[2], environmental chemistry, materials and supramolecular chemistry[5, 6]. Complexes derived from Schiff-bases have pronounced excellent catalytic activities in a variety of process. For instant, metal complexes of Co(II), Fe(III), Ni(II), Cu(II), Zn(II) and Ru(III) complexes with a range of Schiff-bases have shown catalytical activities and have used for carbonylation, hydrogenation, hydroformylation and epoxidation reactions[7-9]. Further, coordination chemistry of Schiff-bases can be applied to tailor a range of metal complexes that have shown a variety of applications in storage devices, sensors, hybrid electronics and optoelectronics[4]. A range of phenoxo- and/or azido-bridged complexes based on Schiff-bases have been fabricated aiming to understanding the magneto-structural and chemical factors that influenced exchange couplin g between metal centres[4]. 2,6-Diformyl-4-methyl-phenol precursor is an interesting versatile moiety that has been used widely by researchers for the formation of a variety of binucleating Schiff-base complexes that have a range of applications[10-12]. Thiadiazole derivatives bearing an important group of heterocyclic compounds that have diverse biological activities, such as anti-tuberculostatic, anti-inûammatory, analgesic, antipyretic, anticonvulsant, antibacterial and antifungal activities[13]. 1,2,4-Triazoles with amino groups on the backbone are potential materials for obtaining various Schiff-base derivatives with well known antimicrobial properties[4]. In the current work we report the formation, spectral investigation and bacterial activity of a range of phenoxo- and azido-bridged complexes with the new multidentate Schiff-base ligand bearing N, O and S donor atoms. The prepared ligand 4'-(((1E,1'E)-(2-hydroxy-5-methyl-1,3-phenylene)bis(methanylylidene))bis(azanylylidene))bis(5-(2-hydroxyphenyl)-2,4-dihydro-3H-1,2,4-tr- iazole-3-thione was derived from the condensation of 2,6-diformyl-4-methyl-phenol and 2-(4-amino-5-mercapto-4H-1,2,4-triazol-3-yl)phenol in a mole ratio 1:2.

EXPERIMENTAL

Materials and methods

All reagents used for the preparation and analysis of compounds were commercially available and used without further purification. Solvents were distilled from appropriate drying agents immediately prior to use. 2,6-Diformyl-4-methyl-phenol and 2-(4-amino-5-mercapto-4H-1,2,4-triazol-3-yl)phenol were prepared by methods published in[14] and[15], respectively.

Physical measurements

Melting points were obtained on electrothermal Stuart apparatus, model SMP30. IR spectra were measured as KBr discs in the range 4000 – 400 cm^{-1} on a Biotech FTIR-600 FTIR spectrometer and CsI discs in the range 4000-250 cm^{-1} on a Shimadzu (FT–IR)–8400S spectrometer. The electronic spectra were recorded in the region 200-1000 nm for 10^{-3} M solutions in DMSO at 25 ºC using a Shimadzu UV-1800 spectrophotometer. ^{1}H- and ^{13}C-NMR spectra were acquired in DMSO-d^6 solution using a Brucker 400MHz spectrometer with tetramethylsilane (TMS) as an internal standard. Mass spectra obtained by positive electrospray technique were recorded on a 5975 QUADROPOLE spectrometer. Elemental analyses (C, H, N and S) were carried out on EuroEA 3000. Metals were determined using a Shimadzu (A A- 7000) atomic absorption spectrophotometer. A Potentiometeric titration method, using a 686-Titro processor-665Dosimat-Metrohm Swiss, was employed to determine chloride content. Conductivity measurements were made with DMSO solutions using a CON 510 digital conductivity meter (Eutech Instruments), and room temperature magnetic moments were measured with a magnetic susceptibility balance (Sherwood Scientific Devised). Thermal analysis

ORIGINAL ARTICLE

(Thermogravimetry (TG), Differential Thermogravimetry (DTG) and Differential Scanning Calorimetry (DSC)) was performed using a Linseis STA PT-1000 TG-DSC instrument.

SYNTHESIS

Preparation to ligand HL

A solution of 2-(4-amino-5-mercapto-4H-1,2,4-triazol-3-yl)phenol (0.25 g, 1.2 mmol) in ethanol (10 ml), was added dropwise with stirring to a mixture of 2,6–diformyl-4–methyl phenol (0.1g, 0.6 mmol) and 4-5 drops of sulfuric acid in ethanol (10 ml). The reaction mixture was allowed to reflux for 3 h, and on cooling at room temperature a solid was formed that filtered under suction. The solid was washed with cold ethanol (5 ml), ether (5 ml) and dried in air. Yield: 1.16 g (89%), m.p= 215-220 °C. IR data (cm^{-1}): 3444 (O-H), 3172 (N-H), 2972 (C-H)$_{aromatic}$, 2860 (C-H)$_{aliphatic.}$, 1633, 1539 and 1383 (C=N)$_{iminic}$, (C=C)$_{aromatic}$ and (C-O)$_{phenolic}$, 1263 (C-S)$_{thion}$. The ^{1}H-NMR spectrum of the ligand in DMSO-d^6 showed peaks at δH; (400MHz, DMSO-d^6): 10.25 (2H, s, O-H), 8.25 (2H, s, H-C=N), 7.60 (2H, m, C4, 4‘-H), 7.20-7.39 (4H, br, C6, 6‘; C_c, $_{c'}$-H), 6.90-7.00 (4H, m, C3, 3‘; C5, 5‘-H), 9.20 (1H, s, OH), 5.00 (2H, s, N-H), 2.75 (3H, s, CH_3). The ^{13}C NMR spectrum of HL in DMSO-d^6 solvent exhibits peaks at δC; (100MHz, DMSO-d^6): 180.50 (C8, 8‘) (C=S), 172.71 (C1, 1‘), 164.45 (C_a), 160.01 (C7, 7‘) (C=N), 155.50 (C9, 9‘) (H-C=N) imine group, (122.01, 142.71, 130.01, 133.72 and 125.11) are assigned for aromatic carbon atoms (C2, 2‘; C3, 3‘; C4, 4‘; C5, 5‘ and C6, 6‘) respectively. (135.45, 121.19 and 120.01) attributed to (C_c; $_{c'}$), (C_d) and (C_b, $_{b'}$)), respectively. 23.50 assigned to (C_e, CH_3). The positive electrospray mass spectrum of HL showed a peak at m/z= 258.2 $(M+2H)^{2+}$ (65%) related to $(M+2H-(H_2N_2))^{2+}$ for $C_{12}H_{12}N_5O_2$, requires= 258.2. Peaks detected at (448/2)= 224 (8.5%), (384/2)= 192 (63%) (320/2)= 160 (70%), (256/2)= 128 (79%), (192/2)= 96 (80%) are related to $(M+2H-(H_2N_2+O_2+N_2))^{2+}$ for $C_{24}H_{24}N_4OS_2$, $(M+2H-(H_2N_2+OHphNN))^{2+}$ for $C_{18}H_{16}N_4O_2S_2$, $(M+2H-(H_2N_2+OHphNN+2S))^{2+}$ for $C_{14}H_{15}N_4O_2$ and $(M+2H-(H_2N_2+OHphNN+C_7H_{15}N_2OS))^{2+}$ for $C_{11}H_{15}N_2O$, respectively. Basic peak that observed at (128/2)= 64 (100%) corresponds to $C_5H_{10}N_2O$.

General synthesis of Schiff-base metal complexes

To a methanolic solution of the Schiff-base ligand (1 mmol) in methanol (15 ml), was added potassium hydroxide (1.1 mmol) dissolved in methanol (10 ml). The mixture was stirred for 10 min, and then a methanolic solution (15 ml) of the metal chloride salt (2 mmol) was added dropwise. The resulting mixture was refluxed under N_2 atmosphere for 2 h, during which time a solid mass was formed that isolated by filtration. The solid was washed with boiling absolute ethanol (10 ml), acetone and dried on air. Elemental analysis data, colours and yields for the complexes are given in (TABLE 1).

^{1}H-NMR spectrum of $K[Zn_2LCl_4]$ in DMSO-d^6 showed peaks at δH; (400MHz, DMSO-d^6): 10.50 (2H, s, O-H), 8.27 (2H, s, H-C=N), 60-7.69 (2H, d, *J*= 7.2Hz, C6, 6‘-H), 7.38 (2H, m, C4, 4‘-H), 7.20 (2H, s, C_c, $_{c'}$-H), 7.00 (4H, m, C3, 3‘; C5, 5‘-H) 5.50 (2H, br, N-H), 2.80 (3H, s, CH_3). ^{13}C-NMR spectrum of $K[Zn_2LCl_4]$ in DMSO-d^6 showed peaks at δC; (100MHz, DMSO-d^6): 190.50 (C8, 8‘) (C=S), 172.61 (C1, 1‘), 177.05 (C_a), 160.05 (C7, 7‘) (C=N), 164.49 (C9, 9‘) (H-C=N) imine group, (135.61, 140.30, 137.17, 138.89 and 136.05) are assigned for aromatic carbon atoms (C2, 2‘; C3, 3‘; C4, 4‘; C5, 5‘ and C6, 6‘), respectively. (139.45, 125.46 and 123.72) attributed to (C_c; $_{c'}$),(Cd) and (C_b; $_{b'}$), respectively. Signal at 21.04 assigned to (C_e, CH_3).

^{1}H NMR spectrum for $[Cd_2LCl_2]Cl(H_2O)$ complex in DMSO-d^6 showed peaks at H; (400MHz, DMSO-d^6): 10.30 (2H, s, O-H), 8.30 (2H, s, H-C=N), 60-7.64 (2H, d, *J*= 3.2Hz, C6, 6‘-H), 7.35 (2H, m, C4, 4‘-H), 7.20 (2H, s, C_c, $_{c'}$-H), 7.00 (4H, m, C3, 3‘; C5, 5‘-H) 4.65 (2H, br, N-H), 2.75 (3H, s, CH_3).

General synthesis of azido-complexes

A solution of sodium azide (10 mmol) in water (5 ml) was added dropwise with stirring, under nitrogen atmosphere, to the title complex (1 mmol) in 15 ml of a mixture of MeOH/DMF (4:1). The reaction mixture was heated at reflux for 3 h. The solid mass that formed was collected by filtration, washed with hot ethanol, acetone and dried in air. Elemental

analysis data, colours and yields for the azido-complexes are given in (TABLE 1).

^{1}H-NMR spectrum of $Na[Zn_2L(N_3)_4](H_2O)_2$ in DMSO-d^6 showed peaks at δH; (400MHz, DMSO-d^6): 10.35 (2H, s, O-H), 8.20 (2H, s, H-C=N), 7.60-7.62 (2H, d, *J*= 1.6Hz, C6, 6‘-H), 7.32 (4H, m, C4, 4‘; C_c, $_{c'}$-H), 6.98 (4H, m, C3, 3‘; C5, 5‘-H), 5.50 (2H, s, N-H), 2.75 (3H, s, CH_3). ^{13}C-NMR spectrum of $Na[Zn_2L(N_3)_4](H_2O)_2$ in DMSO-d^6 showed peaks at δC; (100MHz, DMSO-d^6): 200.10 (C8, 8‘) (C=S), 173.19 (C1, 1‘), 178.76 (C_a), 160.01 (C7, 7‘) (C=N), 165.49 (C9, 9‘) (H-C=N) imine group, (136.04, 145.17, 139.34, 140.72 and 137.46) are assigned for aromatic carbon atoms (C2, 2‘; C3, 3‘; C4, 4‘; C5, 5‘ and C6, 6‘) respectively. (148.72, 130.16 and 125.89) attributed to (C_c, $_{c'}$), (C_d) and (C_b, $_{b'}$), respectively and peak at 23.89 attributed to (C_e, CH_3).

^{1}H-NMR spectrum of $Na[Cd_2L(N_3)_4](H_2O)_2$ in DMSO-d^6 showed peaks at δH; (400MHz, DMSO-d^6): 10.50 (2H, s, O-H), 8.25 (2H, s, H-C=N), 7.45-7.50 (2H, d, *J*= 4Hz, C6, 6‘-H), 7.30 (4H, m, C4, 4‘; C_c, $_{c'}$-H), 6.99 (4H, m, C3, 3‘; C5, 5‘-H), 5.40 (2H, s, N-H), 3.10 (3H, s, CH_3).

Determination of biological activity

Bioactivities were investigated using medium Mueller Hinton agar method[16]. The wells were dug in the media with the help of a sterile metallic borer with centres at least 6 mm. Recommended concentration (100 □ ßL) of the test sample 1mg/mL in DMSO was introduced in the respective wells. The plates were incubated immediately at 37°C for 24 hours. Activity was determined by measuring the diameter of zones showing complete inhibition (mm). To examine the role of DMSO in the biological screening, Separate studies were conducted with the solutions alone of DMSO, which showed no activity against any bacterial strains. Schiff-base ligand and its complexes were found to be potentially active against *Escherichia coli (E. coli), Pseudomonas aeruginosa and Bacillus sabtuius strains*, except ligand that does not exhibit any effects on the activity of *Staphylococcus aureus* bacteria. There is therefore no inhibition zone.

RESULTS AND DISCUSSION

Synthesis and characterisation

The ligand was obtained in a high yield from the reaction of 2,6-diformyl-4-methyl phenol with 2-(4-amino-5-mercapto-4H-1,2,4-triazol-3-yl)phenol in a 1:2 mole ratio. The reaction was carried out in ethanol at reflux, and a multidentate Schiff-base ligand with N_2OS_2 donor atoms was formed according to Scheme (1). The free ligand is soluble with stirring in DMF and DMSO and boiling ethanol and methanol. It is sparingly soluble in other common organic solvents. The ligand and its complexes was characterised by elemental analysis (TABLE 1), IR (TABLE 2) and UV-Vis (TABLE 3) spectroscopy, ^{1}H- and ^{13}C-NMR spectra and mass spectroscopy. The IR spectrum of the free Schiff-base ligand shows characteristic bands at 3444, 3172, 1633, 1539, 1383 and 1263 cm^{-1} attributed to ν(O-H), ν(N-H), $\nu(C=N)_{iminic}$, $\nu(C=C)_{aromatic}$, $\nu(C\text{-}O)_{phenolic}$ and $\nu(C\text{-}S)_{thion}$, respectively[17-19]. The IR spectrum shows no peak around 2600 cm^{-1} may assign to ν(S-H), indicating the ligand exists in thion form (see supporting information, Figure SI 1). The UV-Vis spectrum of HL exhibits an intense absorption peak at 232 nm,

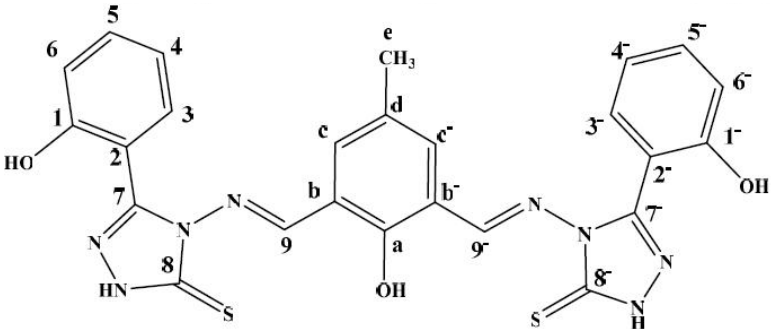

Scheme 1 : Chemical structure of Schiff-base ligand (HL)

ORIGINAL ARTICLE

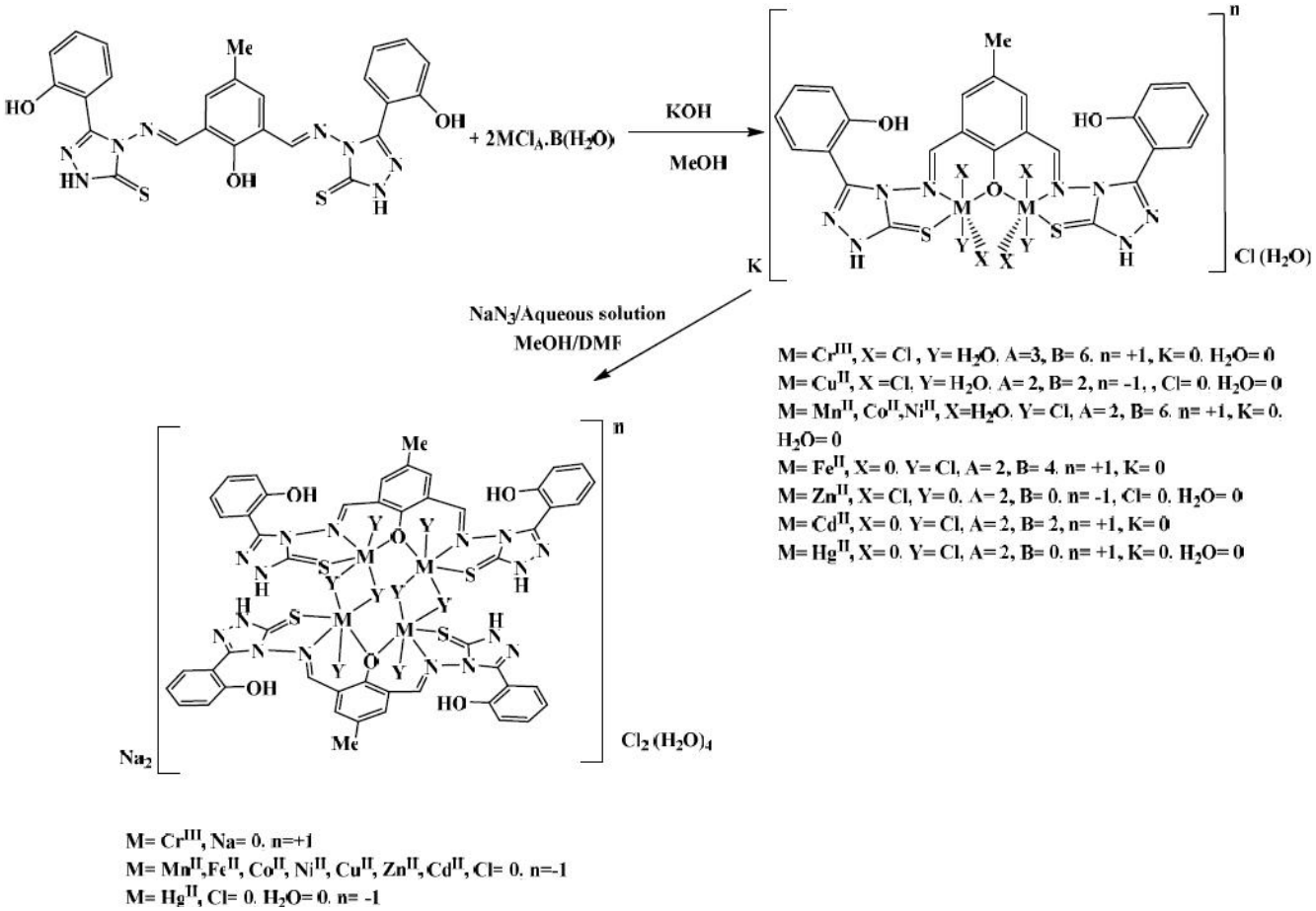

Scheme 2 : Synthesis route and proposed structures of complexes

assigned to $\pi \rightarrow \pi^*$[20]. The peak at 315 nm attributed to $\eta \rightarrow \pi^*$ transition[20].

The phenoxo-bridged binucleating complexes of Schiff-base ligand with Cr(III), Mn(II), Fe(II) Co(II), Ni(II), Cu(II), Zn(II), Cd(II) and Hg(II) were achieved by heating 1 mmol of the ligand with 2 mmol of the metal chloride salt in methanol medium and KOH as a base. The use of KOH facilitates the deprotenation of the ligand, and subsequently assisting in the formation of complexes of the general formula $[Cr_2L(H_2O)_2Cl_4]Cl$, $[M_2L(H_2O)_4Cl_2]Cl$, $K[Cu_2L(H_2O)_2Cl_4]$, $[M'_2LCl_2]Cl(H_2O)$ and $K[Zn_2LCl_4]$ (M= Mn(II), Co(II) and Ni(II); M'= Fe(II) or Cd(II); M'= Hg(II), H_2O= 0) (Scheme 2).

The reactivity studies of the phenoxo-bridged binucleating complexes toward azido moiety were also investigated. The heating of phenoxo-bridged binucleating complexes with NaN_3 in a mixture of $MeOH/H_2O$/DMF resulted in the formation of phenoxo-azido-bridged complexes $[Cr_2L(N_3)_4]Cl(H_2O)_2$ and $Na[M_2L(N_3)_4](H_2O)_2$ (M= Mn(II), Fe(II), Co(II), Ni(II), Cu(II), Zn(II), Cd(II) and Hg(II) (Scheme 2). The complexes, phenoxo-bridged and phenoxo-azido-bridged, are air stable solids, soluble in hot DMF and DMSO, but not soluble in other common organic solvents. The coordination geometries around metal centres were predicted from their physico-chemical analysis. The analytical data (TABLE 1) agree well with the suggested formulae. Conductivity measurements of phenoxo-bridged binucleating complexes in DMSO lie in the 27.45-48.12 $cm^2\ \Omega^{-1}\ mol^{-1}$ range, indicating their 1:1 electrolytic behaviour. The conductivity measurements of phenoxo-azido-bridged complexes in DMSO indicating complexes are electrolyte with a 1:1 nature[21], (see TABLE 1).

FTIR and NMR spectra

The most prominent infrared bands for the complexes together with their assignments are listed in (TABLE 2). The IR spectra of the phenoxo-bridged and phenoxo-azido-bridged complexes exhibited

ORIGINAL ARTICLE

TABLE 1 : Colours, yields, elemental analyses and molar conductance values

Compound	Yield	Colour	m.p. °C	Found, (Calc.)%						ΛM($cm^2\Omega$ mol^{-1})
	(%)			C	H	N	S	M	Cl	
HL	89	Dark yellow	215-220	55.13 (55.14)	3.70 (3.68)	20.58 (20.58)	11.78 (11.76)			
$[Cr_2L(H_2O)_2Cl_4]Cl$	73	Light green	220-224	34.54 (34.92)	2.45 (2.79)	13.00 (13.04)	7.33 (7.45)	12.04 (12.11)	16.12 (20.37)	33.12
$[Mn_2L(H_2O)_4Cl_2]Cl$	83	Red brown	241-244	36.00 (36.10)	3.30 (3.37)	13.40 (13.47)	7.61 (7.70)	13.22 (13.23)	12.54 (12.63)	27.45
$[Fe_2LCl_2]Cl(H_2O)$	75	Dark red	204-207	38.50 (38.51)	2.80 (2.82)	14.32 (14.38)	8.20 (8.21)	14.30 (14.38)	13.12 (13.47)	44.33
$[Co_2L(H_2O)_4Cl_2]Cl$	88	Dark brown	241-243	35.70 (35.75)	3.32 (3.34)	13.24 (13.35)	7.00 (7.63)	14.00 (14.06)	12.44 (12.51)	35.44
$[Ni_2L(H_2O)_4Cl_2]Cl$	72	Light brown	231-234	35.45 (35.75)	3.10 (3.34)	13.22 (13.35)	7.11 (7.63)	13.98 (14.06)	12.45 (12.51)	48.11
$K[Cu_2L(H_2O)_2Cl_4]$	77	Deep brown	270-275	33.64 (33.82)	2.24 (2.71)	12.60 (12.63)	7.20 (7.22)	14.33 (14.43)	15.70 (15.78)	29.12
$K[Zn_2LCl_4]$	92	Orang	263-265	35.10 (35.17)	2.25 (2.34)	13.10 (13.13)	7.40 (7.50)	15.20 (15.24)	16.30 (16.41)	48.12
$[Cd_2LCl_2]Cl(H_2O)$	83	Dark orange	253-255	33.22 (33.67)	2.43 (2.46)	12.52 (12.57)	6.98 (7.18)	24.97 (25.14)	11.33 (11.78)	46.55
$[Hg_2LCl_2]Cl$	62	Orange	246-248	28.50 (28.54)	1.90 (1.91)	10.60 (10.65)	6.08 (6.09)	38.20 (38.24)	9.90 (9.99)	47.67
$[Cr_2L(N_3)_4]Cl(H_2O)_2$	63	Light brown	230-234	33.70 (33.82)	2.65 (2.70)	31.50 (31.57)	7.10 (7.21)	11.68 (11.72)	3.88 (3.94)	31.20
$Na[Mn_2L(N_3)_4](H_2O)_2$	73	Red brown	251-254	33.98 (34.05)	2.25 (2.72)	34.11 (34.22)	7.10 (7.26)	12.33 (12.49)		29.10
$Na[Fe_2L(N_3)_4](H_2O)_2$	65	Dark red	244-247	33.55 (33.98)	2.70 (2.72)	31.70 (31.71)	7.15 (7.24)	12.45 (12.68)		25.70
$Na[Co_2L(N_3)_4](H_2O)_2$	58	Dark brown	251-253	33.39 (33.75)	2.60 (2.70)	31.36 (31.50)	7.14 (7.20)	13.21 (13.27)		32.75
$Na[Ni_2L(N_3)_4](H_2O)_2$	62	Light brown	261-264	33.32 (33.75)	2.68 (2.70)	31.45 (31.50)	7.14 (7.20)	13.15 (13.27)		32.65
$Na[Cu_2L(N_3)_4](H_2O)_2$	57	Deep brown	280-285	33.17 (33.37)	2.60 (2.67)	31.10 (31.15)	7.00 (7.12)	14.10 (14.24)		31.60
$Na[Zn_2L(N_3)_4](H_2O)_2$	72	Dark orange	283-285	33.26 (33.30)	2.54 (2.66)	31.00 (31.08)	7.01 (7.10)	14.40 (14.43)		44.34
$Na[Cd_2L(N_3)_4](H_2O)_2$	63	Dark orange	293-295	30.12 (30.15)	2.20 (2.41)	28.02 (28.14)	6.26 (6.43)	22.31 (22.51)		36.76
$Na[Hg_2L(N_3)_4]$	52	Orange	296-298	26.30 (26.39)	1.53 (1.76)	24.22 (24.63)	5.60 (5.63)	35.26 (35.36)		39.45

ligand bands with the appropriate shifts due to complex formation. Band observed at 1633 cm^{-1} that referred to ν(C=N) of imine group in the free ligand is shifted to lower frequency and appeared around 1614-1622 cm^{-1} in both type of the complexes, pheoxy-bridged complexes and phenoxo-azido-bridged complexes (see supporting information, Figures SI 2 and SI 3). The shift to lower frequency may be related to delocalisation of metal electron density into the ligand π-system. This shift confirmed the coordination of the ligand through nitrogen atoms of imine moieties to the metal ions and indicating strong bonding nature between the metal ions and the iminic (C=N) group[22, 23]. The medium band at 1383 cm^{-1} that due to $\nu(C\text{-}O)_{phenoxo}$ in the free ligand is shifted to higher frequency, upon complexation, and appeared bout 1523-1552 and 1516-1550 cm^{-1} in phenoxo-bridged and phenoxo-azido-bridged complexes, respectively. This shift confirms the involvement of the phenoxo-oxygen atom in the coordination to metal ion in a bridging mode. This is in accordance with previous work reported in literature[23-25]. Furthermore, band at 1263 cm^{-1} that related to ν(C-S) group in the free ligand is shifted to lower

ORIGINAL ARTICLE

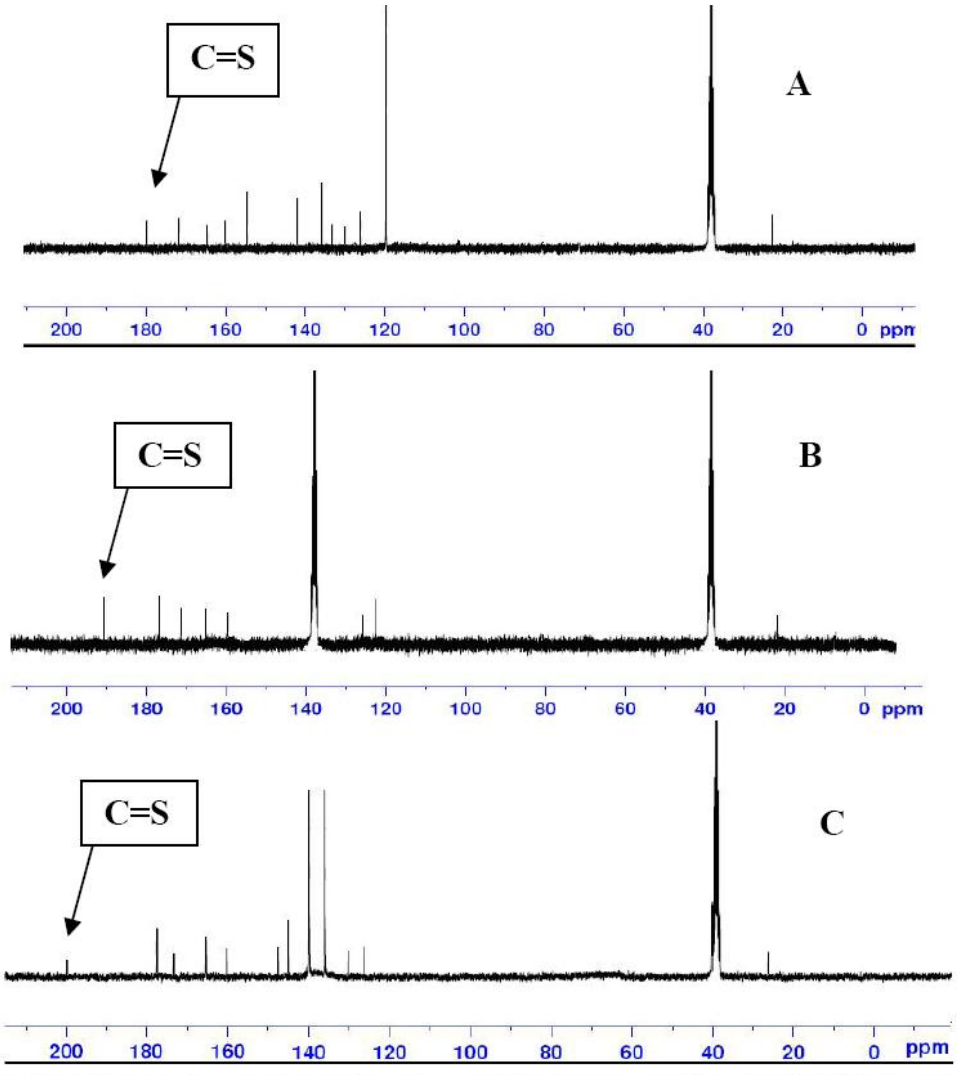

Figure 1 : ^{13}C NMR spectra in DMSO-d6 solutions for: a) HL; b) $K[Zn_2LCl_4]$ and c) $Na[Zn_2L(N_3)_4](H_2O)_2$

frequency and appeared around 1230-1261 cm^{-1} in phenoxo-bridged and phenoxo-azido-bridged. The shift in the ν(C-S) may support the involvement of the sulfur atoms upon complex formation[17, 26]. Band detected at 3172 cm^{-1} that related to ν(N-H) group in the triazole moiety of the free ligand is still existing in the IR spectra of the complexes, appeared around 3200-3369 cm^{-1} in the phenoxo-bridged and phenoxo-azido-bridged complexes. This may indicate the coordination of the ligand to metal ions is in the thion form. The IR spectra of the phenoxo-bridged and phenoxo-azido-bridged complexes show bands in the ranges 536-617, 490-453 and 400-430 cm^{-1} assigned to ν(M-O), ν(M-N) and ν(M-S), respectively[10, 12, 18]. Peaks detected between 254 to 270 cm^{-1} in phenoxo-bridged complexes, attributed to terminally bound chloro ligands ν(M-Cl)[12]. Band attributed to ν(OH) of the aquo group is overlapped with that related to the free (OH) and appeared around 3400 cm^{-1}. Furthermore, the aquo moiety showed additional peaks in the range 1618-1620, 858-900 and 750-780 cm^{-1}, which assigned to $\nu(OH)_{bending}$, $\nu(OH)_{rocking}$ and $\nu(M\text{-}OH_2)$[27], for Schiff-base complexes, receptivity (except complexes Fe(II) and Cd(II), which showed peak around 3400 cm^{-1} assigned to (H_2O) hydrate). The IR spectra of the azido-complexes show peaks around 2044-2100 and 1354-1383 cm^{-1} assigned to asymmetric $\nu_{as}(N_3)$ and symmetric $\nu_s(N_3)$ mode, respectively indicating the bonding of the azido moiety to metal centre[28, 29].

The ^{1}H-NMR spectrum of the free Schiff-base (HL) in DMSO-d^6 solvent shows peak at 8.25 ppm equivalent to two protons that assigned to –CH=N-(imine), indicating the azomethine protons are equiva-

TABLE 2 : FTIR frequencies in (cm^{-1}) of the compounds

Compound	ν (OH)	ν (C=N)	ν(phenoxide)	ν(C=S)	ν(M-O)	ν(M-N)	ν(M-S)	ν(M-Cl)	$\nu_s(N_3)$
HL	$3440_{(br)}$	$1630_{(s)}$	$1383_{(w)}$	1263	-	-	-	-	
$[Cr_2L(H_2O)_2Cl_4]Cl$	$3417_{(br)}$	$1614_{(s)}$	$1525_{(w)}$	1261	573	467	420	265	
$[Mn_2L(H_2O)_4Cl_2]Cl$	$3444_{(br)}$	$1622_{(s)}$	$1552_{(w)}$	1230	553	471	410	260	
$[Fe_2LCl_2]Cl(H_2O)$	$3440_{(br)}$	$1618_{(s)}$	$1543_{(w)}$	1232	523	490	420	250	
$[Co_2L(H_2O)_4Cl_2]Cl$	$3417_{(br)}$	$1610_{(s)}$	$1545_{(w)}$	1238	532	490	410	254	
$[Ni_2L(H_2O)_4Cl_2]Cl$	$3408_{(br)}$	$1622_{(s)}$	$1539_{(w)}$	1250	577	474	425	270	
$K[Cu_2L(H_2O)_2Cl_4]$	$3444_{(br)}$	$1618_{(s)}$	$1550_{(w)}$	1236	553	494	430	254	
$K[Zn_2LCl_4]$	$3433_{(br)}$	$1618_{(s)}$	$1543_{(w)}$	1244	515	471	420	275	
$[Cd_2LCl_2]Cl(H_2O)$	$3444_{(br)}$	$1622_{(s)}$	$1539_{(w)}$	1240	573	478	435	270	
$[Hg_2LCl_2]Cl$	$3452_{(br)}$	$1614_{(s)}$	$1523_{(w)}$	1252	561	519	440	260	
$[Cr_2L(N_3)_4]Cl(H_2O)_2$	$3452_{(br)}$	$1622_{(s)}$	$1535_{(w)}$	1252	561	530	435		$2044_{(s)}$
$Na[Mn_2L(N_3)_4](H_2O)_2$	$3421_{(br)}$	$1618_{(s)}$	$1547_{(w)}$	1232	557	507	428		$2079_{(s)}$ $2112_{(s)}$
$Na[Fe_2L(N_3)_4](H_2O)_2$	$3421_{(br)}$	$1618_{(s)}$	$1543_{(w)}$	1244	515	471	410		$2100_{(s)}$
$Na[Co_2L(N_3)_4](H_2O)_2$	$3429_{(br)}$	$1614_{(s)}$	$1550_{(w)}$	1236	519	420	400		$2067_{(s)}$
$Na[Ni_2L(N_3)_4](H_2O)_2$	$3388_{(br)}$	$1618_{(s)}$	$1543_{(w)}$	1232	523	490	420		$2063_{(s)}$
$Na[Cu_2L(N_3)_4](H_2O)_2$	$3440_{(br)}$	$1610_{(s)}$	$1547_{(w)}$	1225	561	490	410		$2048_{(s)}$ $2089_{(s)}$
$Na[Zn_2L(N_3)_4](H_2O)_2$	$3425_{(br)}$	$1618_{(s)}$	$1547_{(w)}$	1225	565	450	400		$2036_{(s)}$ $2096_{(s)}$
$Na[Cd_2L(N_3)_4](H_2O)_2$	$3448_{(br)}$	$1614_{(s)}$	$1535_{(w)}$	1260	569	467	440		$2046_{(s)}$
$Na[Hg_2L(N_3)_4]$	$3128_{(br)}$	$1610_{(s)}$	$1516_{(w)}$	1244	580	467	430		$2033_{(s)}$

lents. Peaks at 9.20 and 10.25 ppm assigned to O–H groups that derived from 2,d-diformyl-4-methyl-phenol and 2 2-(4-amino-5-mercapto-4H-1,2,4-triazol-3-yl)phenol, respectively. The downfield shift of the latter may be related to intermolecular hydrogen bonding between the O–H groups and to the NMR solvent or it is related to intramolecular hydrogen bonding between sulfur and/or nitrogen atoms of the triazole atoms[10]. The broad signal at δ_H= 7.20-739 ppm equivalent to four protons is related to (C6; 6ˊ,-H) and (C_c; $_{cˊ}$ -H) aromatic protons. The broad appearance is probably due to the relaxation time of the protons, which rely on the frequency applied to measure the resonance. This is in accordance with previous work reported by Al-Jeboori and Al-Shihri[11]. Signal detected at δ_H= 5.00 ppm equivalent to two protons is due to N-H group, indicating that ligand exists in thion form (see supporting information, Figures SI 4). The ^{13}C NMR spectrum in DMSO-d^6 solvent displays peak at δ_c= 180.50 ppm assigned to C=S carbons (Figure 1 a). The ^{1}H and ^{13}C NMR spectra of the free ligand exhibit the other predicted chemical shifts (see experimental, section 3.1).

The ^{1}H-NMR spectra for $K[Zn_2LCl_4]$, $[Cd_2LCl_2]Cl(H_2O)$, $Na[Zn_2L(N_3)_4](H_2O)_2$ and $Na[Cd_2L(N_3)_4](H_2O)_2$ complexes in DMSO-d^6 solvent showed no peak around δ_H= 9.00 ppm may assign to O-H of the phenol group that derived from 2,6-diformyl-4-methyl-phenol precursor, indicating the deprotenation of O-H group upon complex formation. Peak detected at ~ 10.50 ppm equivalent to two protons related to O-H groups, indicating the non-involvement of these groups upon complexation[14]. Signal related to *H*-C=N (imine) group is slightly downfield shifted, appeared at ~ 8.27 ppm. The doublet around 7.60-7.69 ppm equivalent to two protons assigned to (C6; 6ˊ-H) aromatic protons. These protons appear as expected doublet due to rigidity occurred upon complex formation, compared with the broad peak observed in the free ligand. The appearance of (C_c, $_{cˊ}$-H) protons as singlet is related to rigidity occurred in the structure upon complex formation. Protons related to the (N-H) group are shown as singlet at ~ 5.50 ppm (2H, s), indicating complexes exist in thion form (see supporting infor-

ORIGINAL ARTICLE

TABLE 3 : Magnetic moment and UV-VIS spectral data in DMSO solutions

Compound	μeff (BM)	λnm	εmax dm3 mol^{-1} cm^{-1}	Assignment
HL		232	923	$\pi \rightarrow \pi^*$
		315	827	$n \rightarrow \pi^*$
$[Cr_2L(H_2O)_2Cl_4]Cl$	2.91	255	922	$\pi \rightarrow \pi^*$
		353	1321	$n \rightarrow \pi^*$
		368	902	Charge transfer
		676	10	$^4A_2g \rightarrow {}^4T_2g^{(F)}$
$[Mn_2L(H_2O)_4Cl_2]Cl$	6.17	245	2235	$\pi \rightarrow \pi^*$
		335	2029	$n \rightarrow \pi^*$
		345	2306	Charge transfer
		450	78	$^6A_1g \rightarrow {}^4T_2g^{(G)}$
		530	66	$^6A_1g \rightarrow {}^4T_1g^{(G)}$
$[Fe_2LCl_2]Cl(H_2O)$	2.45	274	1987	$\pi \rightarrow \pi^*$
		345	1833	$n \rightarrow \pi^*$
		351	1141	Charge transfer
		550	23	$B_2 \rightarrow E$
$[Co_2L(H_2O)_4Cl_2]Cl$	3.35	267	823	$\pi \rightarrow \pi^*$
		345	1089	$n \rightarrow \pi^*$
		353	1050	Charge transfer
		420	105	$^4T_1g^{(F)} \rightarrow {}^4T_1g^{(P)}$
		715	70	$^4T_1g^{(F)} \rightarrow {}^4A_2g$
$[Ni_2L(H_2O)_4Cl_2]Cl$	4.66	270	1426	$\pi \rightarrow \pi^*$
		371	1233	Charge transfer
		410	43	$^3A_2g \rightarrow {}^3T_1g^{(P)}$
		710	40	$^3A_2g \rightarrow {}^3T_1g^{(F)}$
$K[Cu_2L(H_2O)_2Cl_4]$	1.32	271	2366	$\pi \rightarrow \pi^*$
		622	33	$^2B_1g \rightarrow {}^2B_2g$
$K[Zn_2LCl_4]$	Diamagnetic	272	1901	$\pi \rightarrow \pi^*$
		350	1618	Charge transfer
$[Cd_2LCl_2]Cl(H_2O)$	Diamagnetic	272	1747	$\pi \rightarrow \pi^*$
		351	1342	Charge transfer
$[Hg_2LCl_2]Cl$	Diamagnetic	273	1945	$\pi \rightarrow \pi^*$
		360	1781	Charge transfer
$[Cr_2L(N_3)_4]Cl(H_2O)_2$	7.61	272	1267	$\pi \rightarrow \pi^*$
		350	2011	$n \rightarrow \pi^*$
		361	543	Charge transfer
		470	110	$^4A_2g \rightarrow {}^4T_1g^{(F)}$
		665	35	$^4A_2g \rightarrow {}^4T_2g^{(F)}$
$Na[Mn_2L(N_3)_4](H_2O)_2$	6.98	277	1170	$\pi \rightarrow \pi^*$
		345	2210	$n \rightarrow \pi^*$
		350	422	Charge transfer
		450	95	$^6A_1g \rightarrow {}^4T_2g^{(G)}$
		625	43	$^6A_1g \rightarrow {}^4T_1g^{(G)}$
$Na[Fe_2L(N_3)_4](H_2O)_2$	5.08	270	975	$\pi \rightarrow \pi^*$
		344	1021	$n \rightarrow \pi^*$
		365	1310	Charge transfer
		520	88	$^5T_2g \rightarrow {}^5Eg$
$Na[Co_2L(N_3)_4](H_2O)_2$	6.78	270	1050	$\pi \rightarrow \pi^*$
		340	920	$n \rightarrow \pi^*$
		360	851	Charge transfer
		475	95	$^4T_1g^{(F)} \rightarrow {}^4T_1g^{(P)}$
		610	75	$^4T_1g^{(F)} \rightarrow {}^4A_2g$
$Na[Ni_2L(N_3)_4](H_2O)_2$	2.76	277	786	$\pi \rightarrow \pi^*$
		355	908	$n \rightarrow \pi^*$
		370	675	Charge transfer
		550	91	$^3A_2g \rightarrow {}^3T_1g^{(P)}$
		710	22	$^3A_2g \rightarrow {}^3T_1g^{(F)}$
$Na[Cu_2L(N_3)_4](H_2O)_2$	1.25	265	2014	$\pi \rightarrow \pi^*$
		350	1234	Charge transfer
		630	37	$^2B_1g \rightarrow {}^2B_2g$

Compound	μeff (BM)	λnm	εmax dm3 mol^{-1} cm^{-1}	Assignment
$Na[Zn_2L(N_3)_4](H_2O)_2$	Diamagnetic	272	851	$\pi \rightarrow \pi^*$
		362	894	Charge transfer
$Na[Cd_2L(N_3)_4](H_2O)_2$	Diamagnetic	274	2541	$\pi \rightarrow \pi^*$
		350	1876	Charge transfer
$Na[Hg_2L(N_3)_4]$	Diamagnetic	278	1543	$\pi \rightarrow \pi^*$
		390	1302	Charge transfer

mation, Figures SI 5 - SI 8). The ^{13}C NMR spectra of $K[Zn_2LCl_4]$ and $Na[Zn_2L(N_3)_4](H_2O)_2$ in DMSO-d^6 solvent exhibit peak at 190.50 and 200.10 ppm, respectively assigned to (C8, 8') (C=S) moiety (see Figure 1 b and c, respectively). The significant downfield shift of C=S is due to complexation, compared with that in the free ligand, indicating the involvement of C=S groups in the coordination. The higher downfield shift for the azido-complex may account to the influence of the $(N_3)^-$ moiety, which provides more electron density to the metal centre. The metal centre may delocalise electron density into the ligand π-system (in particular the sulfur dπ-system), and subsequently the C=S exhibits lower bond order and displays more thiol character. Resonance at ~ 178 ppm assigned to phenolic carbon atom (C_a). This chemical shift has showed downfield shift, compared with the free ligand, indicating the involvement of the phenoxo moiety in the coordination. Resonances detected at δ_c= 172.61 and 160.05 ppm attributed to carbon atoms (C1, 1') and (C7, 7') (C=N), respectively. These peaks showed no shift, which indicate the non-involvement of these groups in the coordination. Peak related for the imine moiety appeared at ~ 165 ppm, indicating that the two imine moieties are equivalent and appeared at higher chemical shift compared with the free ligand. This is due to the involvement of the imine groups in complexation.

Mass spectra

The electrospray (+) mass spectrum of the ligand does not show the molecular ion peak. The doubly charged fragment observed at m/z= 258.2 $(M+2H)^{2+}$ (65%) is related to $(M+2H-(H_2N_2))^{2+}$ for $C_{12}H_{12}N_5O_2$, requires= 258.2. Peaks detected at (448/2)= 224 (8.5%), (384/2)= 192 (63%) (320/2)= 160 (70%), (256/2)= 128 (79%), (192/2)= 96 (80%) are related to $(M+2H-(H_2N_2+O_2+N_2))^{2+}$ for $C_{24}H_{24}N_4OS_2$, $(M+2H-(H_2N_2+OHphNN))^{2+}$ for $C_{18}H_{16}N_4O_2S_2$, $(M+2H-(H_2N_2+OHphNN+2S))^{2+}$ for $C_{14}H_{15}N_4O_2$ and $(M+2H-(H_2N_2+OHphNN+C_7H_{15}N_2OS))^{2+}$ for $C_{11}H_{15}N_2O$, respectively. Basic peak that observed at (128/2)= 64 (100%) corresponds to $C_5H_{10}N_2O$ (see supporting information, Figure SI 9).

The electrospray (+) mass spectrum of $K[Zn_2LCl_4]$ exhibits ion peak at m/z= 815.4 $(M+H-(K))^+$ (13.9%) for $Zn_2C_{25}H_{20}N_8O_3S_2Cl_4$, requires= 815.4. Peaks detected at m/z= 677.3 (13.8%), 577.8 (19%), 301.5 (13.7%), 192.2 (82%) and 95.8 (88%) correspond to $(M+H-(K)+(Zn+H_2S+C_2HN))^+$, $[M+H-\{(K)+(Zn+H_2S+C_2HN)+(NO+Cl_2)\}]^+$, $[M+H-\{(K)+(Zn+H_2S+C_2HN)+(NO+Cl_2)+(Zn+4CN+Cl_2+H_2S+H_2)\}]^+$, $[M+H-\{(K)+(Zn+H_2S+C_2HN)+(NO+Cl_2)+(Zn+4CN+Cl_2+H_2S+H_2)+(CN+C_3H_5+CH_4+C_2H_2)\}]^+$ and $[M+H-\{(K)+(Zn+H_2S+C_2HN)+(NO+Cl_2)+(Zn+4CN+Cl_2+H_2S+H_2)+(CN+C_3H_5+CH_4+C_2H_2)+(C_4H_2+O_2+N)\}]^+$, respectively (see supporting information, Figure SI 10).

The electrospray (+) mass spectrum of $Na[Zn_2L(N_3)_4](H_2O)_2$ shows peak at m/z= 842 $(M-(Na+(H_2O)_2))^+$ (10.7%) for $Zn_2C_{25}H_{20}N_{20}O_3S_2$, requires= 842. Peaks detected at m/z= 733.4 (10.5%), 578.1 (34.6 %), 368.8 (14%), 225.5 (34.7%) and 64.2 (100%) correspond to $(M-(Na)+(H_2O)_2+(2CN+C_2H_5N_2))^+$, $[M-\{(Na)+(H_2O)_2+(2CN+C_2H_5N_2)+(Zn+H_2S+2N_2)\}]^+$, $[M-\{(Na)+(H_2O)_2+(2CN+C_2H_5N_2)+(Zn+H_2S+2N_2)+(Zn+4CN+CH+N_2)\}]^+$, $[M-\{(Na)+(H_2O)_2+(2CN+C_2H_5N_2)+(Zn+H_2S+2N_2)+(Zn+4CN+CH+N_2)+(C_4H_7N_4O_2)\}]^+$ and $[M-\{(Na)+(H_2O)_2+(2CN+C_2H_5N_2)+(Zn+H_2S+2N_2)+(Zn+4CN+CH+N_2)+(C_4H_7N_4O_2)+(2CN+CS+OH+2C_2)\}]^+$ respectively (supporting information, Figure SI 11).

The electrospray (+) mass spectrum of $Na[Cd_2L(N_3)_4](H_2O)_2$ shows peak at m/z= 936 $(M-(Na)+(H_2O)_2))^+$ (4.3%) for $Cd_2C_{25}H_{20}N_{20}O_3S_2$, requires= 936. Peaks detected at m/z= 831 (11.8%),

ORIGINAL ARTICLE

TABLE 4 : TGA/DTG/DSC data for ligand (HL), its metal complexes and some azido-complexes

Compound	Stable up to °C	Stage	Decomposition temperature initial-final °C	Nature of transformation/intermediate formed% mass found (calc.)	Nature of DSC peak and temp. °C	DTG peak temp. °C
HL	58	1	58-180	4.925 (5.000)	120 Exo	
		2	190-338	5.2545 (5.300)	212.4 Endo 225 Exo 264.1 Exo 333.2 Endo	242.4
		3	340-463	1.6745 (1.700)	356.4 Exo 359 Endo 446.1 Endo	242.4
		4	465-585	2.8333 (2.800)		
$[Mn_2L(H_2O)_4Cl_2]Cl$	76.1	1	76.1-190	1.4398 (1.500)	105 Exo	
		2	200-330	2.865 (2.900)	231.1 Endo	
		3	340-450	3.898 (3.900)	419.3 Endo	
		4	460-580	3.3237 (3.400)	486.2 Endo	
$[Fe_2LCl_2]Cl(H_2O)$	90	1	90-188	0.3548 (0.3600)	110.6 Exo	
		2	190-323	3.8544 (3.900)	236.7 Endo	
		3	325-378	4.1751 (4.200)	354.6 Endo	361.8
		4	380-538	0.8070 (0.8100)	396.6 Endo 517.5 Exo	
$K[Cu_2L(H_2O)_2Cl_4]$	110	1	81.7-290	3.1493 (3.200)	116 Exo 228.2 Endo	
		2	300-358	5.4387 (5.500)	323.7 Endo	328.5
		3	360-590	1.9128 (2.000)		
$Na[Mn_2L(N_3)_4](H_2O)_2$	94.5	1	94.5-265	5.4423 (5.550)	104 Exo 159 Exo 241 Endo	190
		2	270-440	0.5432 (0.5500)	400.6 Endo	
$Na[Co_2L(N_3)_4](H_2O)_2$	50	1	50-220	1.9571 (2.000)	103 Exo	
		2	250-320	1.2975 (1.3000)		272.7
		3	340-360	0.3716 (0.37200)		336.1
		4	360-480	6.0915 (6.09150)	388.5 Endo 450.3 Endo 510 Endo	397.4
$Na[Ni_2L(N_3)_4](H_2O)_2$	114.7	1	114.7-180	1.5288 (1.5500)	123 Exo	140
		2	190-263	1.7554 (1.800)	235 Exo	
		3	265-590	1.1123 (1.1200)	549.9 Endo	335
$Na[Cu_2L(N_3)_4](H_2O)_2$	98.9	1	98.9-280	5.9314 (6.000)	108.8 Exo 257.6 Endo	240.4
		2	290-440	5.4705 (5.500)	359.5 346 Endo 366 Endo	360
		3	460-540	0.6333 (0.6400)	500.4 Endo	479.6

692.3 (13.9 %), 524 (9.7%), 412.4 (54.8%), 313.7 (39.7%), 141.4 (100%) and 55.4 (97.9%) correspond to $(M-(Na)+(H_2O)_2+(H_2S_2+CN+CH))^+$, $[M-\{(Na)+(H_2O)_2+(H_2S_2+CN+CH)+(Cd+CHN)\}]^+$, $[M-\{(Na)+(H_2O)_2+(H_2S_2+CN+CH)+(Cd+CHN)+(Cd+2N_2)\}]^+$, $[M-\{(Na)+(H_2O)_2+(H_2S_2+CN+CH)+(Cd+CHN)+(Cd+2N_2)+(3CN+H_2O_2)\}]^+$, $[M-\{(Na)+(H_2O)_2+(H_2S_2+CN+CH)+(Cd+CHN)+(Cd+2N_2)+(3CN+H_2O_2)+(C_3H_7N_4)\}]^+$, $[M-\{(Na)+(H_2O)_2+(H_2S_2+CN+CH)+ (Cd+CHN)+$

TABLE 5 : Biological activity for ligand HL, metal complexes and azido-complexes

No.	Sample	Inhibition zone (mm)			
		E. coli	*P. aeruginosa*	*B. sabtuius*	*S. aureus*
1	HL	11	14	8	_
2	Cr-L	9	11	8	6
3	Mn-L	26	11	9	9
4	Fe-L	19	5	10	8
5	Co-L	-	8	10	_
6	Ni-L	16	11	_	5
7	Cu-L	12	19	_	7
8	Zn-L	-	7	_	_
9	Cd-L	14	19	11	10
10	Hg-L	12	9	8	9
11	Cr-azide	18	21	18	16
12	Mn-azide	25	17	19	15
13	Fe-azide	26	13	20	10
14	Co-azide	23	25	26	11
15	Ni-azide	19	29	14	22
16	Cu-azide	16	9	-	21
17	Zn-azide	-	17	18	19
18	Cd-azide	17	23	28	-
19	Hg-azide	30	29	21	10

$(Cd+2N_2)+(3CN+H_2O_2)+(C_3H_7N_4)+(6CN+O)\}]^+$ and $[M-\{(Na)+(H_2O)_2+(H_2S_2+CN+CH)+(Cd+CHN)+(Cd+2N_2)+(3CN+H_2O_2)+(C_3H_7N_4)+(6CN+O)+(CN+2C_2+C)\}]^+$ respectively (supporting information, Figure SI 12).

Electronic spectra and magnetic moment measurements

The electronic spectra and magnetic moments data of the Schiff-base complexes are collected in (TABLE 3). The electronic spectra of the complexes display various peaks around 245-274 and 335-353 nm attributed to $\pi \rightarrow \pi^*$ and $n \rightarrow \pi^*$, respectively. Additional peaks at 345-371 nm assigned to charge transfer (C.T)[30]. The electronic spectrum of the Cr(III) complex showed additional peak at 676 nm assigned to d–d transition type $^4A_2g \rightarrow {}^4T_2g^{(F)}$, indicating a distorted octahedral geometry around metal centre[19]. The magnetic moment value is consistent with octahedral assignment[31]. The electronic spectrum of the Mn(II) complex showed additional d-d transitions peaks at 450 and 530 nm assigned to $^6A_1g \rightarrow {}^4T_2g^{(G)}$ and $^6A_1g \rightarrow {}^4T_1g^{(G)}$, respectively (TABLE 3). The observed magnetic moment is typical for a high-spin binuclear Mn(II) complexes[31, 32]. The $B_2 \rightarrow E$ transition of the Fe(II) complex is detected at 550 nm, which supported the tetrahedral structure around metal centre (supporting information, Figure SI 13). The μ_{eff} value is in agreement with the proposed structure[32]. The electronic spectrum of the Co(II) complex exhibited peaks at 420 and 715 nm that assigned for the $^4T_1g^{(F)} \rightarrow {}^4T_1g^{(P)}$ and $^4T_1g^{(F)} \rightarrow {}^4A_2g$ transitions, respectively (supporting information, Figure SI 14). The Ni(II) complex displays two peaks at 410 and 710 nm, which assigned to $^3A_2g \rightarrow {}^3T_1g^{(P)}$ and $^3A_2g \rightarrow {}^3T_1g^{(F)}$, respectively. The electronic spectra of binucleating Co(II) and Ni(II) complexes and their magnetic moment values is consistent with the distorted octahedral structure. The Cu(II) complex displays a broad band at 622 nm assigned to $^2B_1g \rightarrow {}^2B_2g$ transition. This spectrum and the μ_{eff} value is in agreement with the suggested octahedral geometry. The spectrum of the Zn(II) and Cd(II) complexes exhibited bands assigned to ligand field $\pi \rightarrow \pi^*$ and $M \rightarrow L$ charge transfer[33]. The five-coordinate structure is suggested for the Zn(II) centre[10], while Cd(II) and Hg(II) complexes adopted tetrahedral geometry[10].

ORIGINAL ARTICLE

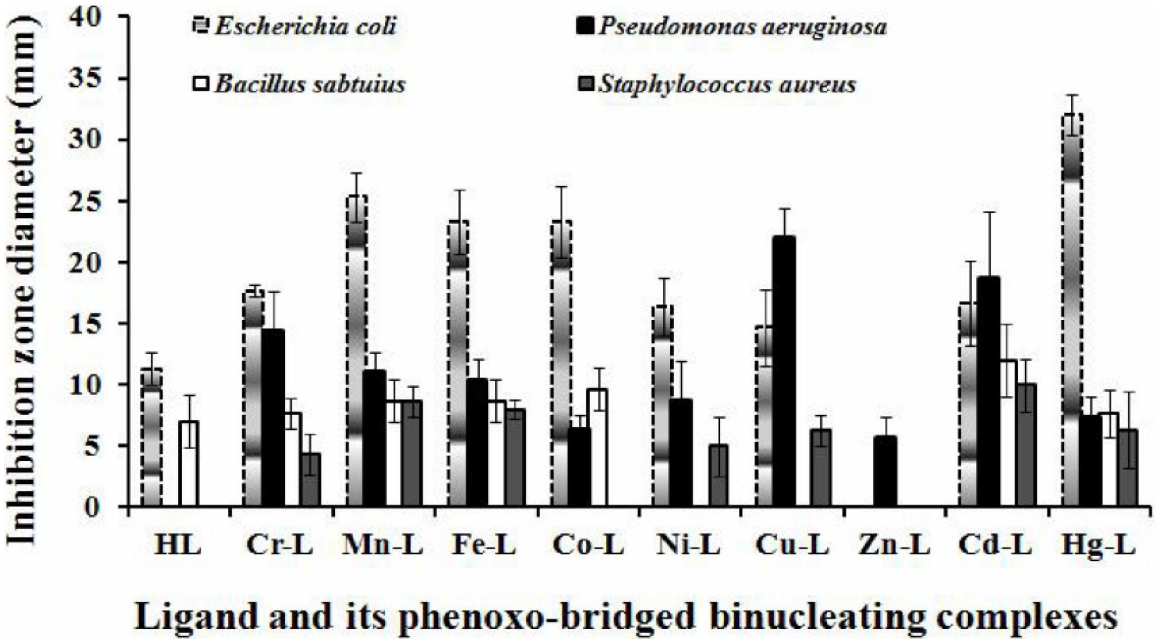

Figure 2 : Evolution of diameter zone (mm) of inhibition of HL and its bimetallic complexes against the growth of various microorganisms. Error bars represent SD between repeated tests

The UV-Vis spectra of azido-complexes exhibit peaks around 265-278 and 340-355 nm attributed to $\pi \rightarrow \pi^{**}$ and $n \rightarrow \pi^{*}$, respectively[20]. Bands detected about 350-390 nm assigned to charge transfer transition (C.T)[27]. The electronic spectrum of the Cr(□II) complex (supporting information, Figure SI 15) showed two additional bands at 470 and 665 nm assigned to $^4A_2g \rightarrow {}^4T_1g^{(F)}$ and $^4A_2g \rightarrow {}^4T_2g^{(F)}$, respectively that could be attributed to the spin allowed d–d transitions[20]. These data together with the magnetic moment 3.8 BM support an octahedral geometry about Cr(III)[34]. The electronic spectrum for Mn(II) displays additional peaks at 450 and 625 nm assigned to $^6A_1g \rightarrow {}^4T_2g^{(G)}$ and $^6A_1g \rightarrow {}^4T_1g^{(G)}$ transition, respectively[10]. The observed magnetic moment is typical for a high-spin binuclear Mn(II) complexes[32]. The $^5T_2g \rightarrow {}^5Eg$ transition of the Fe(□□) complex is detected at 520 nm, which supported the octahedral structure around metal centre. The μ_{eff} value is in agreement with the proposed structure[32]. The electronic spectrum of the Co(II) complex exhibited peaks at 475 and 610 nm assigned for $^4T_1g^{(F)} \rightarrow {}^4T_1g^{(P)}$ and $^4T_1g^{(F)} \rightarrow {}^4A_2g$ transitions. The Ni(II) complex displays two peaks at 550 and 710 nm, which assigned to $^3A_2g \rightarrow {}^3T_1g^{(P)}$ and $^3A_2g \rightarrow {}^3T_1g^{(F)}$, respectively. The electronic spectra of binucleating Co(II) and Ni(II) complex and their magnetic moment values is consistent with the distorted octahedral structure[34]. The Cu(II) complex displays a broad band at 630 nm assigned to $^2B_1g \rightarrow {}^2B_2g$ transition (supporting information, Figure SI 16). This spectrum and the μ_{eff} value are in agreement with the suggested octahedral geometry[31, 32]. The spectrum of the Zn(II), Cd(II) and Hg(II) complexes exhibited bands assigned to ligand field $\pi \rightarrow \pi^{*}$ and M→L charge transfer[10].

The magnetic moment values for the phenoxo-bridged and phenoxo-azido-bridged complexes at (306 K) are lower than the predicted values, indicating the presence of some antiferromagnetic interactions. This may occur from metal-metal interactions through the phenolic oxygen atoms and/or extensive electron delocalisation through azido-bridged group.

Thermal analysis

Thermal analysis data for the ligand (HL) and selected metal complexes are summarised in (TABLE 4). The TG-DSC curves of the ligand and its complexes were determined from ambient temperature to 600˚C in the atmosphere of nitrogen. The analysis of thermal data showed that the ligand is stable up to 58-180 ˚C, where the (C_6H_6O+CH_2S) fragment is lost (obs.= 5.0336 mg; calc.= 5.0699 mg, 25.5%).

ORIGINAL ARTICLE

Peaks detected at 190, 340 and 465 ˚C attributed to the removal of (C_6H_5O+2CN) (obs.= 5.0336 mg; calc.= 5.0699 mg, 26.65%), (CH_2S) (obs.= 1.6745 mg; calc.= 1.6658 mg, 8.5%) and (C_6H_6) (obs.= 2.8329 mg; calc.= 2.8246 mg, 14.38%) molecules, respectively[35, 36]. The final weight (obs.= 4.9089 mg; calc.= 4.8526 mg, 24.91%) represents part of the ligand (sulfur, nitrogen) and carbon residue. The final product is less than the expected weight, which can be related to a partial sublimation during TG analysis (supporting information, Figure SI 17).

The analysis of thermal data of Mn(II), Fe(II) and Cu(II)(II) phenoxo-bridged binucleating complexes appeared to be stable up to 76.1-190 ˚C, where $4H_2O$ molecules is removed (obs.= 1.4398 mg; calc.= 1.3949mg, 8.94%), which indicated presence of $(H_2O)_{aqua}$ molecules that coordinated to Mn(ÀÀ) complex. Peak at 90-188 ˚C attributed to the loss of (H_2O) fragment (obs.= 0.3538 mg; calc.= 0.4067 mg, 2.01%), indicated presence (H_2O) molecules hydrate for Fe(II) complex. For Cu(II) complex peak at 81.7-290 ˚C attributed to the loss of ($2H_2O$+C_6H_6O) fragment (obs.= 3.1479 mg; calc.= 3.0778 mg, 14.99%), indicated presence $(H_2O)_{aqua}$ molecules in the complex. Peaks detected at 200, 190, 300 ˚C attributed to the removal of (CH_3SN+$C_4H_9N_2$) (obs.= 2.865 mg; calc.= 2.8286 mg, 17.79%), (2Cl+$C_2H_6N_3S$) (obs.= 3.8544 mg; calc.= 3.8634 mg, 21.9%) and (2Cl+$C_2H_3N_3S$+CN+SH) (obs.= 5.4387 mg; calc.= 5.4453 mg, 25.89%) for Mn(II), Fe(II) and Cu(II) complexes, respectively. The third step was recorded peaks at 340, 325 and 360 ˚C attributed to the loss of ($C_8H_{12}N_3SO$+H) (obs.= 3.898 mg; calc.= 3.8748 mg, 24.21%), (Cl+2CN+C_2HN_3S) (obs.= 4.1747 mg; calc.= 4.2023 mg, 23.72%) and (NH_2+N_2+C_3H_2) (obs.= 1.9131 mg; calc.= 1.9414 mg, 9.11%) for Mn(II), Fe(II) and Cu(II) complexes, respectively. The final weight loss (obs.= 4.5757 mg; calc.= 4.6112 mg, 28.42%), (obs.= 8.411 mg; calc.= 8.3594 mg, 47.79%) and (obs.= 10.5021 mg; calc.= 10.5355 mg, 50.01%), which attributed for Mn(II), Fe(II) and Cu(II) complexes, respectively (see TABLE 4) represents metallic, nitrogen and carbon residue[35, 36]. The experimental mass loss for the final product is less than the expected weight, which may attribute to a partial sublimation during TG analysis, (supporting information, Figure SI 18 and 19).

The thermal analysis data of Mn(II), Co(II), Ni(II) and Cu(II) for azido-complexes (TG, DTA and DSC) are listed in (TABLE 4). Peaks related to the removal of water molecules hydrate that detected at 94.5-265, 50-220 and 114.7-180 and 98.9-280 ˚C were related to mass loss ($2H_2O$+$2C_8H_7N_3O$+N_2) (obs.= 5.4423 mg; calc.= 5.4424 mg, 43.89%), ($2H_2O$+N_3+CH) (obs.= 2.0354 mg; calc.= 2.034 mg, 10.17%), ($2H_2O$+2CN+CH_3) (obs.= 1.5288 mg; calc.= 1.5288 mg, 11.58%) and ($2H_2O$+$C_8H_9N_4O$+N_3) (obs.= 5.7896 mg; calc.= 5.7892 mg, 28.24%) for Mn(II), Co(II), Ni(II) and Cu(II) azido-complexes, respectively. The second step related for the loss of (C_3H_2) (obs.= 0.5432 mg; calc.= 0.5431 mg, 4.38%), (N_3+CN) (obs.= 1.4744 mg; calc.= 1.474 mg, 7.37%), ($2N_3$+2OH) (obs.= 1.7554 mg; calc.= 1.7554 mg, 13.3%) and ($C_8H_9N_4O$+N_3+CH_3) (obs.= 5.3533 mg; calc.= 5.3526 mg, 26.11%) are detected at 270, 250, 190 and 290 ˚C, which attributed to Mn(II), Co(II), Ni(II) and Cu(II) azido-complexes, respectively. The final weight (obs.= 6.4145 mg; calc.= 6.4322 mg, 51.73%), (obs.= 9.932 mg; calc.= 9.9213 mg, 49.66%), (obs.= 8.8035 mg; calc.= 8.8192 mg, 66.69%) and (obs.= 8.1835 mg; calc.= 8.1863 mg, 39.92%) attributed to Mn(II), Co(II), Ni(II) and Cu(II) azido-complexes, respectively. that represents metallic, nitrogen and carbon residue[35, 36] (see TABLE 4). The experimental mass loss for the final product is less than the expected weight, which may attribute to a partial sublimation during TG analysis, (supporting information, Figure SI 20).

BIOLOGICALACTIVITY

The free Schiff-base ligand and its bimetallic complexes and with Cr(III), Mn(II), Fe(II), Co(II), Ni(II), Cu(II), Zn(II), Cd(II) and Hg(II) ions were screened against Gram negative bacterial strains *Escherichia coli (E. coli), Pseudomonas aeruginosa and Bacillus sabtuius* and Gram positive bacterial strain *Staphylococcus aureus* using disc diffusion method, (TABLE 5). The ligand displays antimicrobial activity against Gram negative strains only. The metal complexes have shown anti-

ORIGINAL ARTICLE

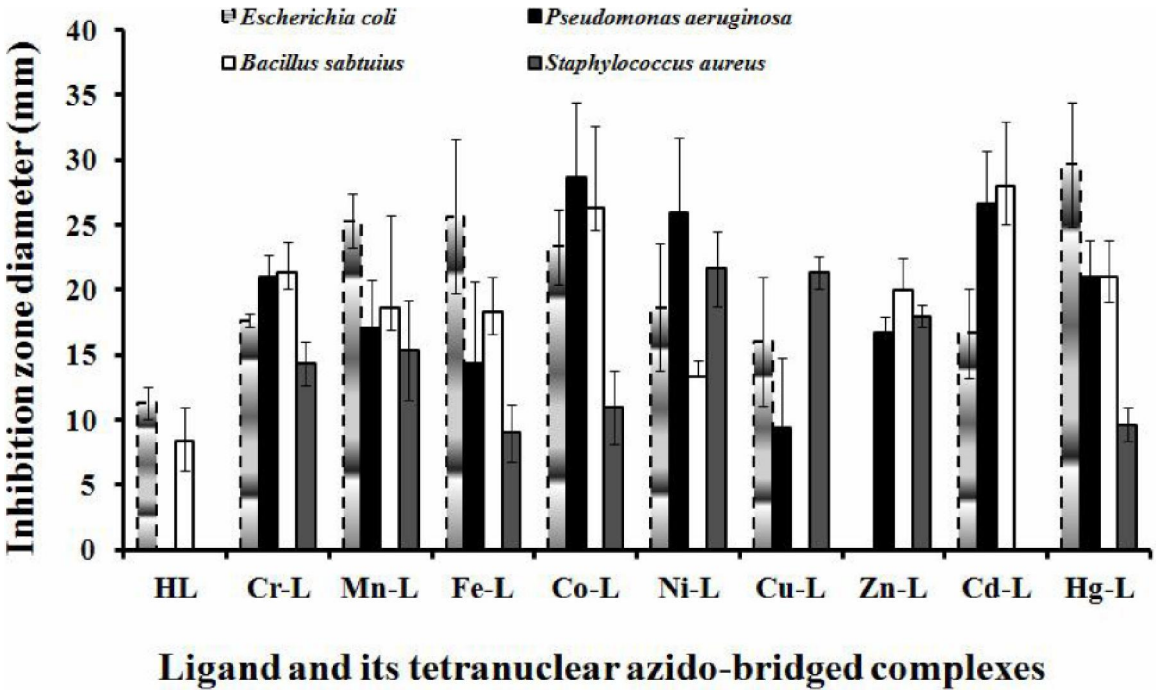

Figure 3 : Evolution of diameter zone (mm) of inhibition of HL and its azido-complexes against the growth of various microorganisms. Error bars represent SD between repeated tests

microbial activity against *Staphylococcus aureus*, compared with the free ligand. Further, complexes Cr(III), Mn(II), Fe(II), Ni(II), Cu(II), Zn(II), Cd(II) and Hg(II) exhibited higher activity against *E. coli*, while complexes Cu(II) and Cd(II) showed more activity against *Pseudomonas aeruginosa*, compared with the free ligand (see Figure 2). The increased activity of the complexes can be discussed on the basis of chelation theory and Overtone's model[37]. According to the chelation approach, complex formation could help the complex to cross a cell membrane of microorganism. This is because chelation significantly decreases the polarity of the metal ion and allowing of the partial sharing of metal positive charge with donor groups. This is can be occurred *via* delocalisation of metal charge into the ligand π-system, over the whole of chelate system. This will increase the lipophilic nature of the metal chelate system which favours its penetration through lipid layer of the cell membranes of microorganism (supporting information, Figure SI 21-24).

As for azido-complexes (TABLE 5), these complexes showed antimicrobial activity against $Gram^-$ and $Gram^+$ strains. Moreover, complexes Cr(III), Mn(II), Fe(II), Co(II), Ni(II), Cu(II), Cd(II) and Hg(II) exhibited higher activity against *E. coli*, while complexes Cr(III), Mn(II), Fe(II), Co(II), Ni(II), Cu(II), Zn(II), Cd(II) and Hg(II) showed more activity against *P. aeruginosa*, compared with the free ligand. Also complexes showed more activity against *B. sabtuius* (see Figure 3). The increased activity of the complexes can be discussed on the basis of chelation theory and Overtone's model[37]. Azido-complexes exhibit higher bacterial activity compared with that prepared from free ligand. This is related to the influence of azido moiety, in which excess of electron is providing to metal ion (supporting information, Figure SI 25-28). This will result in the decreasing of metal positive charge, and subsequently the lipophilic nature of the metal chelate system will be increasing. This should favour the penetration of the complex through lipid layer of the cell membranes of microorganism.

CONCLUSION

In this work we have successfully reported the preparation of a series of phenoxo-bridged complexes using N_2OS_2 donor Schiff-base ligand. The reaction of these complexes with azido moiety gave a double μ-1,1-azido bridged dimeric species. Compounds were characterised using a range of analy-

ses including spectrochemical analyses. The low magnetic measurement values of complexes indicated some antiferromagnetic interaction. The ligand displays antimicrobial activity against Gram negative strains only. However, complexes become more potentially resistive to the microbial activities compared to the free ligand.

REFERENCES

[1] M.Bbadbhade, M.D.Srinivas; Inorg.Chem., **32**, 6122 **(1993)**.

[2] T.Glaser, M.Heidemeier, S.Grimme, E.Bill; Inorg.Chem., **43**, 5192 **(2004)**.

[3] S.Kumar, D.N.Dhar, P.N.Saxena; J.of Scientific and Industrial Research, **68**, 181-187 **(2009)**.

[4] K.Brodowska, E.Ł.Chruscinska; Chemik, **68(2)**, 129-134 **(2014)**.

[5] J.M.Lehn; Supramolecular chemistry concepts and perspectives, 1st Edition, Wiley-**VCH**, Weinheim, **(1995)**.

[6] B.Belghoul, W.Welterlich, A.Maier, A.Toutianoush, A.Rabindranath, T.B.Langmuir; **23**, 5062 **(2007)**.

[7] A.G.Asuero, M.J.Navas, J.M.Bautista, D.Rosales; Microchemical Journal, **28(2)**, 183 **(1983)**.

[8] J.Dehand, J.Jordanov, A.Mosset; J.Galy.Inorg.Chem., **18**, 1543 **(1979)**.

[9] K.J.Oberhausen, J.F.Richandon, R.M.Buchanan; Inorg.Chem., **30**, 1357 **(1991)**.

[10] M.J.Al Jeboori, H.A.Hassan, W.A.J.Al-Sa'idy; Transition Met Chem., **34**, 593-598 **(2009)**.

[11] M.J.Al Jeboori, A.S.Al Shihri; J.Saudi Chem.Soc., **5(3)**, 341 **(2001)**.

[12] F.H.Al-Jebooria, M.J.Al-Jeboorib, K.K.Hammuda, H.I.Ashoura, J.M.Mohammada; Journal of Chemical and Pharmaceutical Research, **5(4)**, 160-170 **(2013)**.

[13] M.Du, X.J.Zhao; J.Mol.Struct., **694**, 235 **(2004)**.

[14] P.H.Smith, J.R.Morris, G.D.Ryan; J.Am.Chem.Soc., **111**, 7437 **(1989)**.

[15] A.J.Atkins, A.J.Blake, M.Scheoder; J.Chem.Soc.Chem.Commun, 353 **(1993)**.

[16] A.U.Rahman, M.I.Choudhary, W.J.Thomsen; Bioassay techniques for drug development, harwood academic, Amsterdam, The Netherlands, **(2001)**.

[17] K.J.Oberhausen, J.F.Richandon, R.M.Buchanan; Inorg.Chem., **30**, 1357 **(1991)**.

[18] Z.Wang, J.Reibenspies, E.M.Arthur; Inorg.Chem., **36**, 629-636 **(1997)**.

[19] W.Low; phys.Rev., 109 **(1958)**.

[20] M.J.Al Jeboori, A.J.A.Ghani, A.J.Al Karawi; Transition Met.Chem., **33**, 925-930 **(2008)**.

[21] W.J.Geary; Coordination Chemistry Reviews, **7(1)**, 81-122 **(1971)**.

[22] H.Koksal, M.Tumer, S.Serin; Inorg.Met.Org.Chem., **26**, 1577 **(1996)**.

[23] P.H.Smith, J.R.Morris, G.D.Ryan; J.Am.Chem.Soc., **111**, 7437 **(1989)**.

[24] M.Tumer, C.Celik, H.Koksal, S.Serin; Transition Met.Chem., **24**, 525 **(1999)**.

[25] J.Dehand, J.Jordanov, A.Mosset; J.Galy.Inorg.Chem., **18**, 1543 **(1979)**.

[26] J.R.Shah, M.S.Patil; J.Indian Chem.Soc.LV, **3**, 944 **(1981)**.

[27] M.J.Al Jeboori, A.H.Al Dujaili, A.E.Al Janabi; Transition Met.Chem., **34**, 109-113 **(2009)**.

[28] A.D.Khalaji, H.S.Evans; Polyhedron, **28**, 3769-3773 **(2009)**.

[29] P.P.Chakrabarty, S.Giri, D.Schollmeyer, H.Sakiyama, M.Mikuriya, A.Sarkar, S.Saha; Polyhedron, **89**, 49-54 **(2015)**.

[30] A.B.P.Lever; Inorganic Electronic Spectroscopy, New York, **(1984)**.

[31] Z.Guo, G.Li, L.Zhou, S.Su, Y.Li, S.Dang, H.Zhang; Inorg.Chem., **48**, 8069 **(2009)**.

[32] P.Albores, E.Rentschler; Inorg.Chem., **49**, 8953-8961 **(2010)**.

[33] N.N.G.wood, A.Earnshow; J.Wiley and sons Inc., **9**, 314 **(1998)**.

[34] A.Z.El-Sonbati, A.S.Al-Shihri, A.A.El-Bindary; Spectrochemica Acta Part A., **60**, 1763 **(2004)**.

[35] H.Arora, F.Lloret, R.Mukherjee; Eur.J.Inorg.Chem., 3317-3325 **(2009)**.

[36] Q.Chen, M.H.Zeng, L.Q.Wei, M.Kurmoo; Chem.Mater, **22**, 4328-4334 **(2010)**.

[37] R.V.Singh, R.Dwivedi, S.C.Joshi; Transition Metal Chemistry, **29(1)**, 70-74 **(2004)**.